Soft, adhesive (+) alpha tocopherol phosphate planar bilayers that control oral biofilm growth through a substantive antimicrobial effect

Harper, Robert; Saleh, Mais M; Carpenter, Guy; Abbate, Vincenzo; Proctor, Gordon; Harvey, Richard D ; Gambogi, Robert J; Geonnotti, Anthony; Hider, Robert; Jones, Stuart A

DOI:
10.1016/j.nano.2017.12.024

ELSEVIER

Nanomedicine: Nanotechnology, Biology, and Medicine
xx (2018) xxx – xxx

nanomedicine
Nanotechnology, Biology, and Medicine

nanomedjournal.com

Soft, adhesive (+) alpha tocopherol phosphate planar bilayers that control oral biofilm growth through a substantive antimicrobial effect

Robert A. Harper, PhD[a,1], Mais M. Saleh, MPharm[a], Guy Carpenter, PhD[b], Vincenzo Abbate, PhD[a], Gordon Proctor, PhD[b], Richard D. Harvey, PhD[d], Robert J. Gambogi, PhD[c], Anthony Geonnotti, PhD[c], Robert Hider, PhD[a], Stuart A. Jones, PhD[a,*]

[a]*King's College London, Institute of Pharmaceutical Science, Franklin-Wilkins Building, London, UK*
[b]*King's College London, Dental institute, Division of Mucosal & Salivary Biology, Tower Wing, Great Maze Pond, London, UK*
[c]*Johnson and Johnson, Consumer & Personal Products Worldwide Division of Johnson & Johnson Consumer Companies, Inc, Skillman, NJ, USA*
[d]*Martin-Luther-Universität Halle-Wittenberg, Institute of Pharmacy, Halle (Saale), Germany*

Received 10 August 2017; accepted 27 December 2017

Abstract

'Soft' nanomaterials have the potential to produce substantive antibiofilm effects. The aim of this study was to understand the oral antimicrobial activity of soft nanomaterials generated from alpha-tocopherol (α-T) and alpha-tocopherol phosphate (α-TP). (+) α-TP formed planar bilayer islands (175 ± 21 nm, −14.9 ± 3.5 mV) in a Trizma® buffer, whereas (+) α-T formed spherical liposomes (563 ± 1 nm, −10.5 ± 0.2 mV). The (+) α-TP bilayers displayed superior *Streptococcus oralis* biofilm growth retardation, a more substantive action, generated a superior adsorption to hydroxyapatite and showed an enhanced inhibition of multi-species bacterial saliva biofilm growth (38 ± 7μm vs 58 ± 18 μm, P □ 0.05) compared to (+) α-T. Atomic force microscopy data indicated that the ability of the 'soft' α-TP nanomaterials to transition into planar bilayer structures upon contact with interfaces facilitated their adhesive properties and substantive antimicrobial effects.

Key words: Nanomaterials; Tocopherol phosphate; Vitamin E; Biofilm; Antimicrobial; Soft; Streptococcus; Penetration; Growth; Oral cavity; Teeth

The ability of synthetic nanomaterials to impair bacterial adhesion, dismantle biofilms and kill microorganisms has been established using solid nanosized particles.[1–4] However, there is a lack of information about how 'soft' nanomaterials, e.g. liposomes, act as antimicrobial agents.[5] Soft nanomaterials can elicit antimicrobial effects, in a similar manner to solid nanomaterials, through physical surface interactions with microorganisms, but in addition, soft nanomaterials can also induce an intercellular antimicrobial effect if they are fabricated from antimicrobial agents that are released from the nanomaterial in the presence of the microorganisms. Further research is needed to understand how both the surface properties and composition of soft nanomaterials influence their antimicrobial action such that these materials can be used effectively.

In the oral cavity, where microbial biofilm control is needed to maintain good oral health, the ability of soft nanomaterials to act as effective antimicrobials has been demonstrated.[6] However, the saliva that flows into the mouth and down the throat, thus constantly washing the oral surfaces, limits the contact of the soft nanomaterials with their target microorganisms and thus their efficacy. It is possible that soft nanomaterials can be fabricated to display properties which facilitate penetration into biofilms, adhesion to teeth and a substantive antimicrobial action though the slow release of the antimicrobial used to form the nanomaterial, but to achieve this new soft nanomaterials are needed.[7,8]

Funding information: The study was financed by an Engineering and Physical Sciences Research Council (EPSRC) CASE award with Johnson and Johnson. EPSRC had no role in study design, data collection and interpretation, or the decision to submit the work for publication. Johnson and Johnson had a role in some experimental design and data interpretation.

*Corresponding author at: King's College London, Institute of Pharmaceutical Science, Franklin-Wilkins Building, London, SE1 9NH.
E-mail address: stuart.jones@kcl.ac.uk (S.A. Jones).
[1] Currently at: School of Dentistry, University of Birmingham, UK.

https://doi.org/10.1016/j.nano.2017.12.024

The aim of this study was to understand the antimicrobial activity of soft nanomaterials generated from alpha-tocopherol (α-T) and alpha-tocopheryl phosphate (α-TP). α-T shows some surface activity in aqueous solvents where it forms liposomes, but when phosphorylated to produce alpha-tocopheryl phosphate (α-TP) the phosphate of α-TP will be charged, which enables it to bind charged surfaces, e.g., teeth.[9] Through the comparison of the physical properties (size, charge, shape, architecture, surface chemistry and rigidity of their aggregates in water) of α-T and α-TP and their interactions with bacteria in biofilms it was anticipated that a better understanding of the antimicrobial effects of soft nanomaterials could be gained. The nanomaterials in this work were generated from plant extracted (+) α-T to produce a naturally derived product.[10,11] The morphology of the nanomaterials was assessed by AFM rather Cryo-TEM as this deposited the materials on a surface and mimicked their adsorption in the mouth. *Streptococcus oralis* and *Streptococcus mutans* were selected as the principle target organisms because in oral health applications it is important for substantive antimicrobial agents to have good activity against early tooth colonizers to prevent and delay biofilm development.

Materials

(+) α-T (Type VI, ~40% purity), phosphorus oxychloride ($POCl_3$) (≥ 99%), tetrahydrofuran (THF) (anhydrous) (≥ 99.9%), triethylamine, Trizma® hydrochloride (≥ 99%), Tween 80, lecithin, triflouroacetic acid (TFA) (≥ 99%), deuterated chloroform ($CDCl_3$), C18 silica, chlorhexidine digluconate (CHX) 20 % (w/v) in water, brain heart infusion (BHI) broth and glycerol were purchased from Sigma Aldrich, UK. Hexane fractions (60-80), propan-2-ol, methanol, formic acid (FA), absolute ethanol, disodium hydrogen phosphate, monosodium dihydrogen phosphate, blood agar (BA) plates containing blood agar base no. 2 with 5 % horse blood, hydrochloric acid, sodium hydroxide and sterile 0.2 μM nylon syringe filters were purchased from Fisher Scientific Ltd, UK. All chemicals were reagent grade unless otherwise specified. De-ionized water was used from laboratory supply. *S. oralis* NCTC 7864T was purchased from LGC standards, USA. Hydroxyapatite disks (HA) (5 mm diameter × 2 mm thick) were purchased from Himed Inc, USA. Mica was purchased from Agar scientific, Elekron technology, UK. AFM cantilevers which were uncoated Si_3N_4 probes with integrated pyramidal tips (Model: NSC15/noAl) were purchased from MikroMasch, Germany. Disposable clear dynamic light scattering cuvettes (macro, PMMA) and disposable folded capillary cells (DTS1070) were purchased from VWR, Germany. Clear sterile polyester adhesive films were purchased from Starlab, UK. Live/dead BacLight™ bacterial viability kit, for microscopy, was purchased from Life Technologies, UK.

Methods

Synthesis and characterization of (+) α-TP

The natural, non-commercially available isoform of (+) α-TP was synthesized by adding a (+) α-T (3.0395 g, 7.057 mmol) anhydrous THF (25 mL) solution to a mixture of triethylamine (2.854 mL, 20.47 mmol, 2.9 equivalence) and phosphorus oxychloride (1.973 mL, 21.17 mmol, 3 equivalence) in anhydrous THF (15 mL) under nitrogen at room temperature (3 h). The white triethylamine hydrochloride powder (side product) was removed (suction filtration), distilled water (75 mL) was added to the mixture, it was allowed to stir for 24 h and triple hexane extraction was performed. The first hexane extraction was with the reaction mixture (product in the hexane layer), the second with disodium hydrogen phosphate (10 mM, 50 mL, pH 10.8, product in polar layer) and the third with acidified disodium hydrogen phosphate (2M, 20 mL). The crude (+) α-TP product (0.7221 g, 50.1%, Figure 1) was purified using a C18 silica packed column (30 cm × 3 cm) with a 70% propan-2-ol, 30% water, 0.1% TFA mobile phase.

^{1}H, ^{13}C and ^{31}P nuclear magnetic resonance (NMR) spectra were collected to confirm the (+) α-TP product's structure using a DRX 400 instrument (Bruker, UK) in $CDCl_3$ at 296 K with a 5 mm switchable broadband probe. The NMR structural information was supported by mass spectra recorded using a micromass ZQ 2000 instrument (Waters, UK), operating in negative electrospray ionization (ESI) mode. The sample was directly infused into the mass spectrometer's ESI source at a 20 μl/ min flow rate from a 100 μg/ mL sample solution prepared in 50% methanol, 50% water and 0.1% FA. Circular dichroism (CD) samples were measured on an Applied Photophysics Spectrophotometer (Leatherhead, UK) with a photodiode detector (Avalon, UK) using a CDDC channel at 1000 V. Wavelengths were measured from 180 to 400 nm taking a reading every 1 nm with a bandwidth of 2 nm.

HPLC was used to assess the product purity and chemical degradation rates using a Phenomenex, Luna C8 column and mobile phase that consisted of 70% propan-2-ol, 30% water and 0.1% TFA. There was no analytical standard for (+) α-TP to calculate purity; hence, this was estimated as a percentage of total peak area in the chromatogram. The chemical degradation rates of (+) α-TP and (+) α-T (20 μg/ mL, 39 μM) when dispersed in a 20% ethanol, 80% water at pH 7.4 (Trizma® buffer, 25 mM) were calculated over a 12 week period.

Characterization of (+) α-T and (+) α-TP nanomaterials

The critical packing parameter was used to predict aggregate structure in the vehicle. It was calculated from v_o/ael_o as previously described.[12] The (+) α-TP ae value used was 54 $Å^2$.[13,14] An ae value for (+) α-T was not found in the literature. Height and phase images of the untreated mica, the Trizma® vehicle (20% ethanol, 80% water, 150 mM Trizma® at pH 7.4), the (+) α-T (0.15% w/v) and the (+) α-TP (0.15% w/v) dispersed in 20% ethanol, 80% water at pH 7.4 with and without 150 mM Trizma® were recorded on an AFM (Bruker icon dimension, UK). All images were obtained in tapping mode using high resonance frequency (harmonic resonance frequency = 320 kHz) pyramidal cantilevers with uncoated Si_3N_4 tips displaying force constants of 46 N/m in air. Mica was chosen as a solid substrate on to which 2-3 drops of the test samples were placed; the samples were dried with nitrogen and then imaged. Scan speeds were set at 0.9 Hz. Measurements were recorded using the

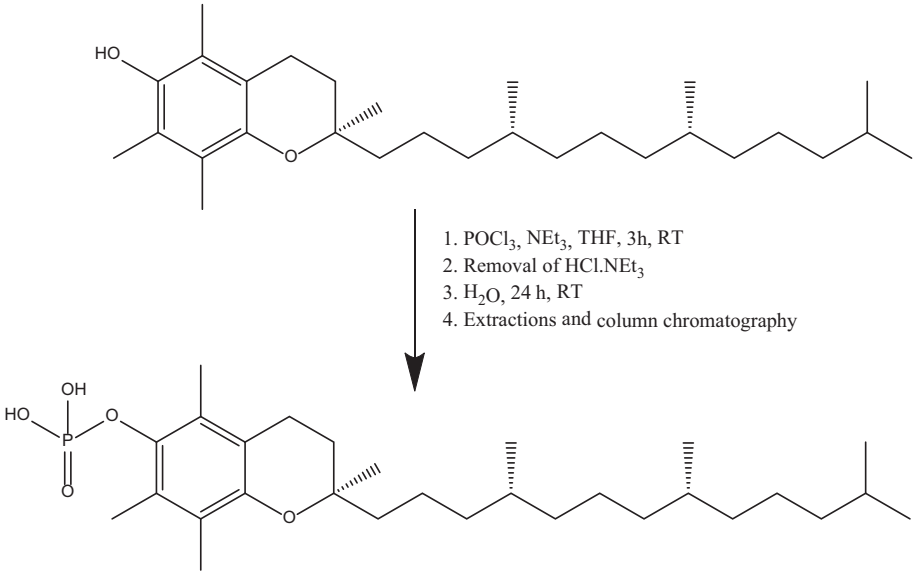

Figure 1. Chemical synthesis of (+) alpha tocopheryl phosphate from (+) alpha tocopherol.

NanoScope 1.50 AFM image analysis software (Bruker, USA) and were analyzed using Gwyddion 2.45, a free SPM data visualization and analysis program.

The (+) α-TP nanoaggregate size, zeta potential and critical aggregation constant (CAC) were analyzed by photon correlation spectroscopy (Malvern Nanoseries Zetasizer, Malvern Instruments Ltd, UK) at 173° with a temperature of 25 °C. All the (+) α-TP samples were dissolved in 20% ethanol 80% water solvent systems buffered at pH 7.4 ± 0.2 with Trizma® (25 mM). Blank solutions (containing just solvent) and (+) α-TP (100 μM) solutions were assessed for aggregation 18 h after sample preparation by monitoring the non-attenuated derived count rate (Kcp) and size (nm) in triplicate.

Streptococci biofilm antimicrobial growth retardation assay

S. oralis NCTC 7864T and *S. mutans* NCTC 10449T were cultivated on blood agar (BA) plates containing blood agar base no. 2 and 5% horse blood, at 37 °C under aerobic conditions. Plates were subcultured every 48 h and passaged no more than 6 times. The cell suspensions were used after 2 controlled growth cycles in broth and centrifugal sedimentation on to a 96-well microtiter plate. Test solutions were applied for 2 min, washed off with saline and growth was monitored in fresh BHI at 37 °C in a UV-Vis plate reader for 24 h. The Richards model was used to interpret the growth curves.[15] The time to inflection point was the mid-point of exponential growth phase.[16] The post-growth maximum population density was the optical density at which the bacterial growth curves plateaued.[17] The doubling time was calculated from a linear function applied to the exponential phase of the *S. oralis* growth curves.

To understand if (+) α-TP was binding to the cell surfaces of *S. oralis,* the antimicrobial growth retardation assay was performed and the cells exposed to the test solutions were washed twice with a neutralizing rinse (200 μL) instead of saline. The neutralizing rinse consisted of Tween 80, 10% (v/v), lecithin, 0.5% (w/v), and phosphate buffer (281 μM pH 7.2 ± 0.2) in distilled water.

MBC assay

The MBCs were assessed on the best performing compounds in order to benchmark the test substances with other established antimicrobial agents. *S. oralis* and S. mutans were cultured as previously described with the 24 h broth culture then diluted to 4 × 10^5 CFU/mL and plated at 100 μL/well in 96 well plates with the test solutions (100 μL). After 24 h at 37 °C, 100 μL aliquots from each well were transferred to blood agar plates and the plates were incubated for 24 h at 37 °C. The blood agar plates were then assessed for colony formation along with controls.

Unstimulated whole mouth saliva biofilm growth inhibition

To form a multispecies biofilm, HA disks pre-treated with (+) α-TP (0.15% w/v, 300 μL) or (+) α-T (0.15% w/v, 300 μL) for 10 min were washed with saline (600 μL, 2 min), placed vertically in unstimulated whole mouth saliva (UWMS) (400 μL) in micro centrifuge tubes and incubated at 37 °C for 18 h (without supplements). The UWMS was collected from one donor that had fasted for at least 8 h by spitting into a falcon tube (15 mL). The saliva was vortexed before aliquots were taken. The saliva itself was not treated, but incubated with tocopherol treated HA disks to monitor biofilm attachment/growth. After the 18 h incubation the HA disks were then washed with saline (600 μL, 2 min) and exposed to the live/dead stain (200 μL) for 30 min followed by imaging. Biofilms were observed using 10× oil immersion objective and a SP2 confocal microscope (Leica,UK) with 488 and 568 nm excitation. Green fluorescence (500-530 nm) represented uptake of Syto 9 by live cells and red fluorescence (> 620 nm) represented uptake of propidium iodide by dead cells. There was no crossover between emission spectra

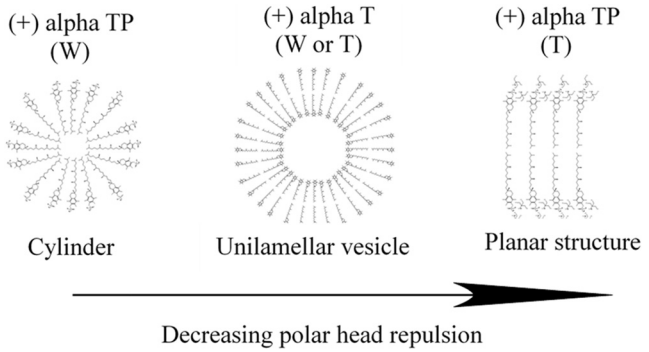

Figure 2. Nanostructure shape transition scheme where (+) alpha T is (+) alpha tocopherol, (+) alpha TP is (+) alpha tocopheryl phosphate. (W) is a 20% ethanol, 80% water vehicle and (T) is a 20% ethanol, 80% water, 150 mM Trizma®, pH 7.4 vehicle.

and excitation intensities were ≤ 31%. Biofilms grown on HA disks pre-treated with the test sample vehicle were used as controls. Experiments were performed by measuring biofilm height once, on each side of each HA disk using three different disks by measuring Z-stacks from the biofilm surface to the hydroxyapatite surface. All images were taken from the center of each disk.

Hydroxyapatite binding assay

HA disks were placed into micro centrifuge tubes containing (+) α-TP or (+) α-T test solutions (0.01% w/v, 300 μL in 20% ethanol, 80% water, pH 7.4 with 150 mM Trizma® vehicle) statically for 10 min. Disks were then removed and placed in saline (600 μL) for 2 min and then the test agent was quantified by HPLC as described previously.

Statistical analysis

All values were expressed as their mean ± standard deviation (SD). Statistical analysis was performed using Levine's homogeneity test to ensure all sample group data were close to an acceptable normal distribution ($P > 0.05$) before statistical significance between the sample groups was assessed by one way analysis of variance (ANOVA) tests with post-hoc Tukey analysis in Origin 2016. Statistically significant differences were assumed when $P \leq 0.05$.

Results

Synthesis and characterization of (+) α-TP

The structure of (+) α-TP (obtained with a 27% yield and 99% purity (by HPLC), see supplementary materials, Figure S1) was confirmed by the presence of a single phosphorus NMR peak at −1.27 ppm (See supplementary materials, Figure S2, *A*), 29 carbon NMR peaks (see supplementary materials, Figures S2, *B*, S3 and Table S1) and the aromatic methyl group chemical shifts of (+) α-T and (+) α-TP, which indicated that the conversion from (+) α-T to (+) α-TP was successful (see supplementary materials, Figure S2, *C*). The naturally derived (+) α-TP showed a mass of 509.3, (*i.e.*, $[M\text{-}H]^-$, see supplementary material, Figure S4), which when compared with the calculated M/Z of the (+) α-TP free acid (510.4 g/mol) confirmed the formation of the phosphorylated product. CD data of the product in conjunction with its C^{13} NMR data confirmed the natural stereochemistry of the structure was retained during the synthesis (see supplementary material, Figure S5). The chemical degradation rate was 1.2 μg/ mL/week for (+) α-TP and 4.75 μg/ mL/week for (+) α-T (see supplementary material, Figure S6).

Biophysical analysis of the nanomaterials

The calculated critical packing parameter for (+) α-TP was 0.50 and this suggested that (+) α-TP would form cylindrical micelles or spherical liposomes in this work. The ae value for (+) α-T could not be found, but it was predicted to be smaller than (+) α-TP due to a reduction in head group polarity, thus the packing parameter > 0.5, which suggested (+) α-T was more likely to form spherical liposomes or planar bilayers in this work (Figure 2).

AFM imaging substantiated the theoretical calculations as they showed (+) α-T formed spherical liposomes with diameters of 551 ± 43 nm and a height of ~86 nm (Figure 3, *A*) and the (+) α-TP formed cylindrical micelles (Figure 3, *B*) with a height of ~22 nm. The addition of Trizma® to the vehicle did not influence the (+) α-T structure (See supplementary material, Figure S7), but the (+) α-TP transitioned from the cylindrical micelles to planar bilayer islands, which displayed heights of ~4.6 nm (Figure 3, *C*). The height of the bilayer islands matched with the theoretical length of two (+) α-TP molecules, end to end, which supported the bilayer structure (See supplementary material, Figure S8, *A* and *B* for controls). The AFM phase images showed that the (+) α-TP planar bilayer islands where viscoelastic, exhibiting adhesion to the silicon nitride cantilever probes (more so than the cylindrical micelles, See supplementary material, Figure S9), but (+) α-T liposomes were not.

The CAC of (+) α-TP was found to be 5.5 ± 0.2 μM 18 h after preparation (Figure 4, *A*). At 0.1 mM, 0.005% w/v the hydrodynamic size of the planar bilayer islands was 175 ± 21 nm; they were shown to have a slight negative charge of −14.9 ± 3.5 mV, a PDI value of 0.359 ± 0.06 and a unimodal size distribution (Figure 4, *B*).

The z-average diameter of the (+) α-T spherical liposomes at a concentration of 0.1 mM (56044 ± 175 kcps) was 563 ± 1, they had a small negative charge of −10.5 ± 0.2 mV, a PDI value of 0.179 ± 0.03 and a unimodal size distribution (see supplementary material Figure, S10). The (+) α-TP planar bilayer islands were found to be stable over 8 days; the size and polydispersity index of the nanomaterials remained the same ($P > 0.05$) (Figure 5, *A* and *B*).

Substantive antimicrobial growth retardation of (+) α-T and (+) α-TP against S. oralis biofilms

S. oralis biofilms displayed a growth time inflection point at 2.2 ± 0.9 h when treated with water for 2 min and 1.7 ± 0.2 h (Figures S12 and 6) with Trizma® ($P > 0.05$); this corresponded to a doubling time of 0.17 h. An increase of the growth time inflection point to approximately 11 h was observed when *S. oralis* was treated with the positive control CHX at a concentration of 0.01% (a doubling time of 1.54 h). (+) α-TP was found to retard *S. oralis* bacterial by up to 5.4 ± 1.3 h (a

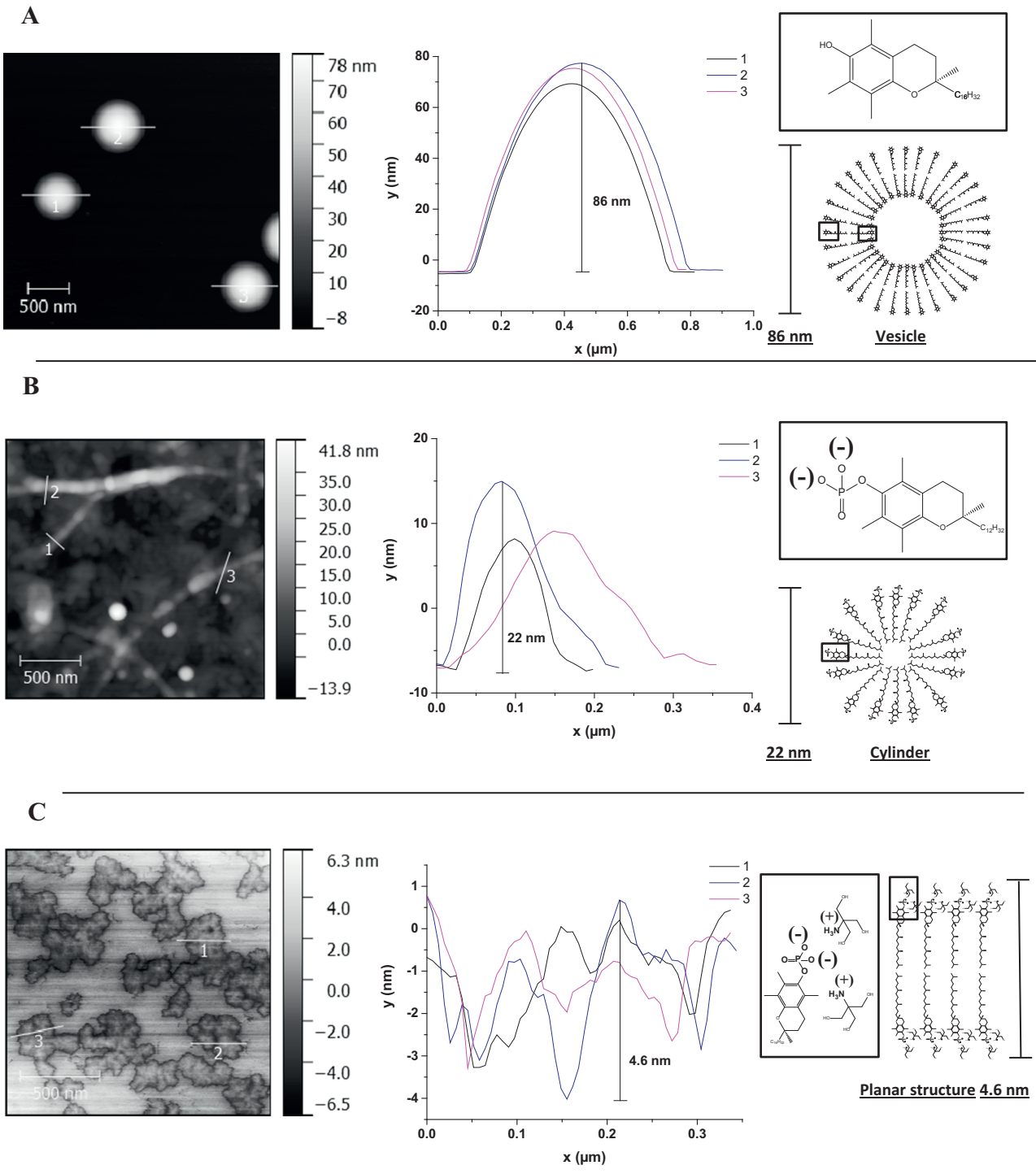

Figure 3. Atomic force microscopy tapping height images (left), cross-sectional profile (middle) and molecular packing (right) with enlarged head group inset. **(A)** (+) alpha tocopherol, **(B)** (+) alpha tocopheryl phosphate, **(C)** (+) alpha tocopheryl phosphate with Trizma® (150 mM). Three lines on the cross sectional are shown, one from each of three repeat measurements.

doubling time of 0.78 h at a concentration of 0.51%, Figure 6). (+) α-T (0.43% w/v, 10 mM) gave a very small, statistically significant, inhibition of *S. oralis* growth at 2.0 ± 0.3 h ($P < 0.05$, doubling time of 0.18 h). The maximum population density of *S. oralis* after the treatment with (+) α-TP was reduced in a dose dependent manner (Figure 6, $P < 0.05$), but CHX showed little effect with increasing concentration until a dramatic reduction in microorganism population density when using a 0.01% w/v solution ($P < 0.001$). For CHX there appeared to be a correlation between increased time to inflection point and reduced maximum population density; however, this was not the case for (+) α-TP.

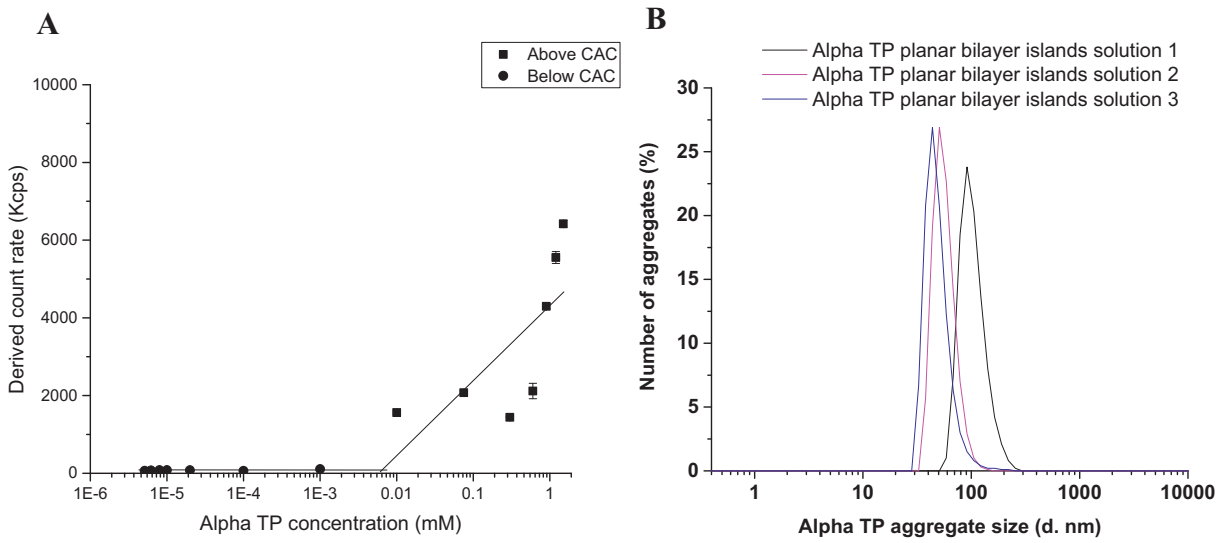

Figure 4. Dynamic light scattering derived critical aggregate concentration calculation (CAC) **(A)** and aggregate size distribution (0.1 mM) **(B)** of (+) alpha tocopheryl phosphate in 20% ethanol, 80% water at pH 7.4 ± 0.2 (25 mM Trizma®) (n =3).

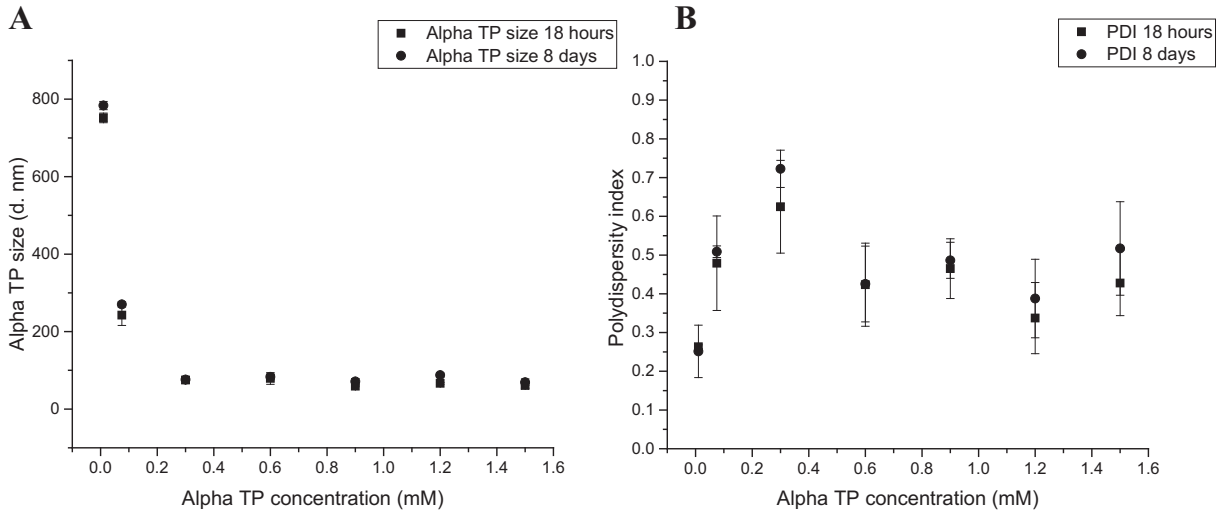

Figure 5. (+) alpha tocopheryl phosphate dynamic light scattering size **(A)** and polydispersity index **(B)** at 18 h and 8 days.

When *S. oralis* was washed with a charge neutralizing rinse instead of saline after the application of test solutions CHX no longer gave a dose dependent response in growth inhibition and its overall activity was suppressed (Figure 7). This effect was mirrored when the (+) α-TP treated bacteria were washed with the neutralizing rinse (Figure 7) as (+) α-TP also no longer gave a dose dependent response in growth inhibition and its overall activity was also suppressed.

(+) α-TP was less effective against *S. mutans (growth inflection point - 3.0 ± 0.5 h)*, but it did statistically inhibit growth rate ($P = 0.01$) and maximum population density ($P < 0.001$) (See supplementary material, Figure S13, *A* and *B*).

Minimum bactericidal concentration

(+) α-TP (in the Trizma® vehicle) when diluted in the broth culture resulted in turbidity and so the visible growth of bacteria could not be monitored in order to determine the minimum inhibitory concentration using a traditional methodology. However, the MBC was found to be 1 μg/ mL for *S. oralis* (See supplementary material, Figure S14) and >512 μg/ mL for *S. mutans*.

Unsterilized whole mouth saliva biofilm growth inhibition of (+) α-T and (+) α-TP

Confocal imaging (See supplementary material, Figure S15) showed that HA disks pre-treated with the vehicle produced a biofilm height of 76 ± 15 μm (Figure 8, *A*). Disks pre-treated with (+) α-T (3 mM) resulted in a biofilm height of 58 ± 18 μm, which was not statistically different to the vehicle control ($P > 0.05$). HA disks pre-treated with (+) α-TP (3 mM, 0.15% w/v) resulted in a biofilm of 38 ± 7 μm in height, which was significantly smaller compared to the vehicle control ($P = 0.0006$) and (+) α-T ($P < 0.05$) pre-treated disks.

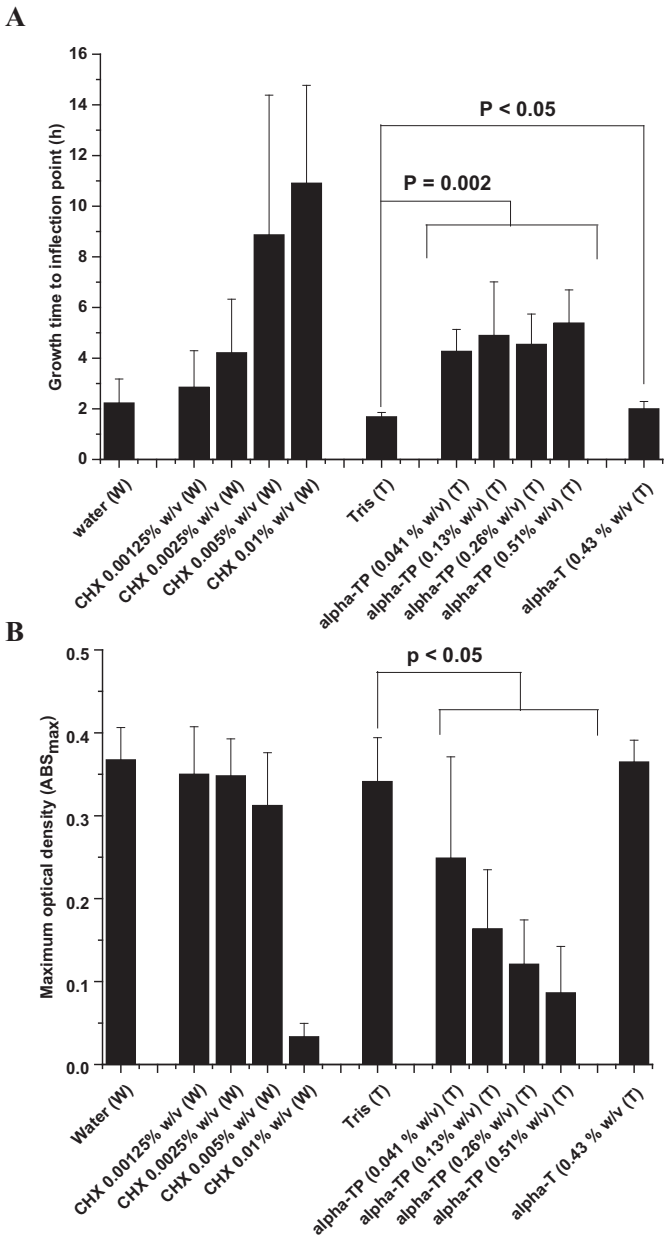

Figure 6. **(A)** Time to growth inflection points of Streptococcus oralis and **(B)** post-growth maximum population densities when washed with saline. CHX is chlorhexidine, alpha TP is (+) alpha tocopheryl phosphate and alpha T is (+) alpha tocopherol. Data represent mean ± standard deviation (n=3). (Tris (T) consists of 20% ethanol, 80% water (v/v) with 150 mM Trizma® at pH 7.4 ± 0.2) (Water (W) contains 20% ethanol). ABS: absorbance at 620 nm.

Binding of (+) α-T and (+) α-TP to hydroxyapatite

The (+) α-TP remaining in the fluid after incubation with the HA disk was 25% ± 12% of its initial concentration (Figure 8, *B*). Using the same molar concentration of (+) α-T, 99% ± 18% was found in the incubation fluid, which suggested that it did not to bind to HA. The difference in (+) α-TP and (+) α-T HA binding was statistically different ($P = 0.00006$). Attempts to wash the (+) α-TP off the HA using saline were not successful.

Discussion

(+) α-TP was less susceptible to oxidation and formed cylindrical micelles in water whilst (+) α-T formed spherical liposomes. This aligned with previous work with α-tocopheryl polyethylene glycol succinate 1000 (α-TS).[18,19] Using Trizma® in the dispersion vehicle forced the (+) α-TP nanomaterials to transition from elongated micelles to planar bilayer islands. This was thought to be due to the Trizma® ion-pairing with the

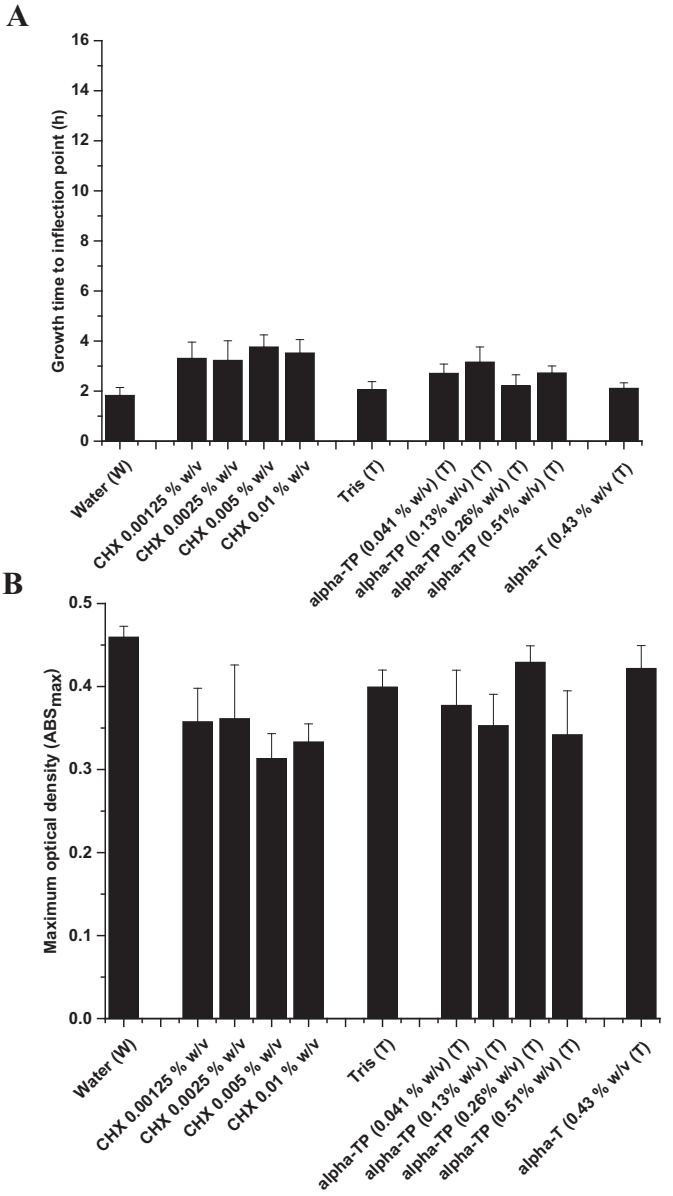

Figure 7. **(A)** Time to growth inflection points of *Streptococcus oralis* biofilms treated then washed with neutralizing rinse and **(B)** post-growth maximum population densities. CHX is chlorhexidine, alpha TP is (+) alpha tocopheryl phosphate and alpha T is (+) alpha tocopherol. Data represent mean ± standard deviation (n=3) (Tris (T) consists of 20% ethanol, 80% water (v/v) with 150 mM Trizma® made pH 7.4 ± 0.2) (Water (W) contains 20% ethanol). ABS: absorbance at 620 nm.

negatively charged phosphate group of (+) α-TP and consequentially reducing the polar head repulsion in the aggregate. This ion-pairing did not occur when the (+) α-TP was dispersed in the deionized water/ ethanol solution due to the very low number of counter-ions available in the dispersion solution. Whether the planar bilayers existed in solution in the same form as when they were deposited on a solid surface, as in the AFM experiments, was not clear from the data, but in this work their shape when interacting at an interface, either the tooth or the micro-organisms, drove their biological activity and hence it was used to define their shape.

The planar bilayer islands, despite ion-pairing with Trizma® to dampen the –ve surface charge, were the most adhesive of the nanomaterials when imaged in the AFM studies. This suggested that the shape of the aggregate played an important role in its adhesive properties. The planner bi-layers were flatter and thus displayed a larger surface area than the other aggregate structures and this would generate more points of contact with microorganisms and tooth surfaces. It is accepted that AFM images from which the aggregate adhesion was calculated were collected using a silicon nitride probe (Si_3N_4), but the probes did display similar physicochemical properties to the hydroxyapatite ($Ca_{10}(PO_4)_6(OH)_2$) disks.[20]

The (+) α-T and (+) α-TP nanomaterials displayed similar hydrodynamic diameters in light scattering experiments and the AFM images. They also generated a micromolar CAC, which

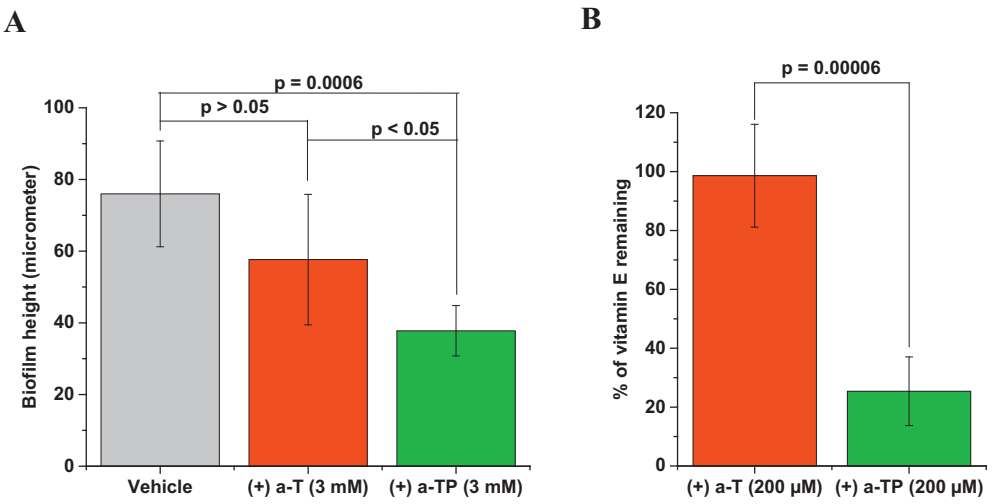

Figure 8. **(A)** Height of oral biofilms formed on hydroxyapatite pre-treated disks and **(B)** amount of (+) a-T and (+) a-TP remaining in solution after 10 min exposure to hydroxyapatite disks. (+) a-T was alpha tocopherol, (+) a-TP was (+) alpha tocopheryl phosphate and the vehicle was 20% ethanol, 80% water, 150 mM Trizma®, pH 7.4. Data represent mean ± standard deviation (n=3).

suggested that at concentrations relevant to their use as an oral health care product the agents would form nanomaterials with good physical stability.[21] This was supported by the sizing data over a period of 18 h. Good physical stability is a trait of planar bilayer structures[22] and it was these nanomaterials that effectively inhibited the micro-organism growth. The maximum optical densities of the controls and the growth inhibition were in the same range as previous work with zinc.[23] In addition, the (+) α-TP planar bilayer nanomaterials seemed to show good activity compared to Listerine™.[24] Therefore, in the context of the previously published work (+) α-TP planar bilayers display reasonable antimicrobial efficacy. This conclusion was supported by the *S. oralis* MBC of (+) α-TP (1 μg/ mL), which was lower than CHX (7.8 μg/ mL),[25] cetylpyridinium chloride (7.8 μg/ mL) and triclosan (5.2 μg/ mL),[26] all antimicrobial agents that act *via* cell lysis.[27,28] The low MBC for (+) α-TP suggested that it acted via an intracellular mechanism. It is a potent signaling molecule that targets enzymes including acid and alkaline phosphatases, adenosinetriphosphatase, diphosphopyridine nucleotidase[29] and transcription factors.[30] Moreover, it has been suggested that (+) α-TP directly binds and regulate mRNAs encoding enzymes involved in its biosynthesis controlling gene expression.

The superior activity of the (+) α-TP planar bilayers against *S. oralis* compared to *S. mutans* was thought to be a consequence of the *S. mutans* showing less favorable interactions with the nanomaterials.[31] The neutralizing rinse studies supported this hypothesis by showing the substantive effect was related to active adsorption of the (+) α-TP planar bilayers to the biofilm in a similar manner to CHX.[32] This substantive antimicrobial action, the AFM adhesion data and the HA adsorption data demonstrated that the shape and the surface phosphate groups (PO_4^{2-}) of (+) α-TP were important in its ability to control oral bacteria growth and bind to calcium within the teeth. However, the (+) α-TP planar bilayers did not form a physical barrier to completely inhibit biofilm growth, rather the (+) α-TP killed a proportion of the micro-organisms that formed a biofilm on the hydroxyapatite and this in turn controlled biofilm growth. Controlling the oral micro-organism bioburden, rather than completely eradicating it, is the goal of maintaining good oral health; therefore these data suggested that (+) α-TP could be an effective oral healthcare active.[33] Biofilm control is the main challenge in addressing two of the world's most common diseases: dental caries and periodontitis. Both are characterized by biofilms which become resistant to daily tooth brushing in part because the biofilms secrete extracellular matrices. Thus although controlling the bacterial load is important, future treatments need to also target established biofilms. This paper demonstrates (+) α-TP, which is a naturally occurring compound, has bacteriostatic and biofilm penetration properties with the added benefit that it binds strongly to teeth (hydroxyapatite) to maintain effective concentrations in similar way as the current market leader CHX.

Appendix A. Supplementary data

The data supporting this research are openly available from http://doi.org/10.18742/RDM01-266. Supplementary data to this article can be found online at https://doi.org/10.1016/j.nano.2017.12.024.

References

1. Paula AJ, Koo H. Nanosized building blocks for customizing novel antibiofilm approaches. Journal of Dental Research. *Crit Rev Oral Biol Med* 2016:1-9.
2. Arakha M, Saleem M, Mallick BC, Jha S. The effects of interfacial potential on antimicrobial propensity of ZnO nanoparticle. *Sci Rep* 2015;**5**9578.
3. Wei QS, Ji J, Fu JH, Shen JC. Norvancomycin-capped silver nanoparticles: synthesis and antibacterial activities against E-coli. *Sci China Ser B: Chem* 2007;**50**(3):418-24.

4. Choi KH, Nam KC, Lee SY, Cho G, Jung JS, Kim HJ, et al. Antioxidant potential and antibacterial efficiency of caffeic acid-functionalized ZnO nanoparticles. *Nanomaterials* 2017;**7**(6):148.
5. Zhuang X, Mai Y, Wu D, Zhang F, Feng X. Two-dimensional soft nanomaterials: a fascinating world of materials. 2015;**27**(3):403-27.
6. Dong D, Thomas N, Thierry B, Vreugde S, Prestidge CA, Wormald P-J. Distribution and inhibition of liposomes on Staphylococcus aureus and Pseudomonas aeruginosa biofilm. *PLoS ONE* 2015;**10**(6):e0131806, https://doi.org/10.1371/journal.pone.0131806.
7. Ganesan K. Ph.D. thesis. University of Duisburg-Essen, Germany. *Functionalization of calcium phosphate nanoparticles with organic phosphates*; 2008.
8. Meers P, Neville M, Malinin V, Scotto AW, Sardaryan G, Kurumunda R, et al. Biofilm penetration, triggered release and in vivo activity of inhaled liposomal amikacin in chronic Pseudomonas aeruginosa lung infections. *J Antimicrob Chemother* 2008;**61**:859-68.
9. Wa FK, Gebicki JM. Oxidation of α-tocopherol in micelles and liposomes by the hydroxyl, perhydroxyl, and superoxide free radicals. *Arch Biochem Biophys* 1983;**226**(1):242-51.
10. Moddresi M. Ph.D. thesis. London College of Fashion, University of the Arts London, London, UK. *The use of nanotechnology in enhancing the efficacy of cosmetic actives of natural origin*; 2010.
11. Ogru E, Gianello R, Libinaki R, Smallridge A, Bak R, Geytenbeek S, et al. Vitamin E Phosphate: an endogenous form of vitamin E. Free radicals and oxidative stress: chemistry, biochemistry and pathophysiological implications. *Meeting of the Society for Free Radical Research Ioannina, Greece, June 26-29*; 2003. p. 127-32.
12. Nagarajan R. Molecular packing parameter and surfactant self-assembly: the neglected role of the surfactant tail. *Langmuir* 2002;**18**:31-8.
13. Chevalier Y, Chachaty C. NMR investigation of the micellar properties of monoalkylphoshpates. *Colloid Polym Sci* 1984;**262**:489-96.
14. Ravoo BJ, Engberts JBFN. Single-tail phosphates containing branched alkyl chains. Synthesis and aggregation in water of a novel class of vesicle-forming surfactants. *Langmuir* 1994;**10**:1735-40.
15. Dalgaard P, Koutsoumanis K. Comparison of maximum specific growth rates and lag times estimated from absorbance and viable count data by different mathematical models. *J Microbiol Methods* 2001;**43**:183-96.
16. Mackay BJ, Denepitiya L, Iacono VJ, Krost SB, Pollark JJ. Growth-inhibitory and bactericidal effects of human parotid salivary histidine-rich polypeptides on Streptococcus mutans. *Infect Immun* 1984;**4**(3):695-701.
17. Fine DH, Furgang D, Lieb R, Korik I, Vincent JW, Barnett ML. Effects of sublethal exposure to an antiseptic mouthrinse on representative plaque bacteria. *J Clin Periodontol* 1996;**23**(5):444-51.
18. Sadoqi M, Lau-Cam CA, Wu SH. Investigation of the micellar properties of the tocopheryl polyethylene glycol succinate surfactants TPGS 400 and TPGS 1000 by steady state fluorometry. *J Colloid Interface Sci* 2009;**333**(2):585-9.
19. Muthu MS, Kulkarni S, Liu Y, Feng SS. Development of docetaxel-loaded vitamin E TPGS micelles: formulation optimization, effects on brain cancer cells and biodistribution in rats. *Nanomedicine* 2012;**7**(3):353-64.
20. An YH, Friedman RJ. *Handbook of bacterial adhesion: principles, methods, and applications*. New York: Humana Press Inc., Springer Science + Business Media; 2000.
21. Wanga J, Suna J, Chena Q, Gaoa Y, Lia L, Lia H, et al. Star-shape copolymer of lysine-linked di-tocopherol polyethylene glycol 2000 succinate for doxorubicin delivery with reversal of multidrug resistance. *Biomaterials* 2012;**33**(28):6877-88.
22. Wu H, Su K, Guan X, Sublette ME, Stark RE. Assessing the size, stability and utility of isotropically tumbling bicelle systems for structural biology. *Biochim Biophys Acta* 2010;**1798**(3):482-8.
23. Gan SY. PhD thesis, King's College London. *Antimicrobial activity of zinc chelator complexes*; 2010.
24. Fine DH, Furgang D, Lieb R, Korik I, Vincent JW, Barnett ML. Effects of sublethal exposure to an antiseptic mouth rinse on representative plaque bacteria. 1996;**23**(5):444-51.
25. Wang BY, Hong J, Ciancio SG, Zhao T, Doyle MP. A novel formulation effective in killing oral biofilm bacteria. *J Int Acad Periodontol* 2012;**14**(3):56-61.
26. McBain AJ, Ledder RG, Sreenivasan P, Gilbert P. Selection for high-level resistance by chronic triclosan exposure is not universal. *J Antimicrob Chemother* 2004;**53**:772-7.
27. McBain AJ, Bartolo RG, Catrenich CE, Charbonneau D, Ledder RG, Gilbert P. Effects of a chlorhexidine gluconate-containing mouthwash on the vitality and antimicrobial susceptibility of in vitro oral bacterial ecosystems. *Appl Environ Microbiol* 2003;**69**:4770-6.
28. Haps S, Slot DE, Berchier CE, Van der Weijden GA. The effect of cetylpyridinium chloride-containing mouth rinses as adjuncts to toothbrushing on plaque and parameters of gingival inflammation: a systematic review. *Dent Hyg* 2008;**6**:290-303.
29. Zingg JM, Meydani M, Azzi A. α-Tocopheryl phosphate — an active lipid mediator? *Mol Nutr Food Res* 2010;**54**:679-92.
30. Gianelo R, Libinaki R, Azzi A, Gavin PD, Negis Y, Zingg JM, et al. Alpha-tocopheryl phosphate: a novel, natural form of vitamin E. *Free Radic Biol Med* 2005;**39**:970-6.
31. Saito T, Takatsuka T, Kato IT, Ishihara K, Okuda K. Adherance of oral streptococci to an immobilised antimicrobial agent. *Arch Oral Biol* 1997;**42**(8):539-45.
32. Elworhy A, Greenman J, Doherty FM, Newcombe RG, Addy M. The substantivity of a number of oral hygiene products determined by the duration of effects on salivary bacteria. *J Periodontol* 1996;**67**:572-6.
33. Marsh PD. Role of the oral microflora in health. *Microb Ecol Health Dis* 2000;**12**:130-7.